OPTOELECTRONICS AND ADVANCED MATERIALS – RAPID COMMUNICATIONS Vol. 9, No. 11-12, Nov. – Dec. 2015, p. 1514 - 1519

Synthesis of CuO-ZnO and its application in photocatalytic degradation of nonylphenol polyethoxylate

M. GIAHI*, H. TAGHAVI, S. SAADAT[a], A. ABDOLAHZADEH ZIABARI[a]
Department of Chemistry, Lahijan Branch, Islamic Azad University, Lahijan, Iran
[a]*Department of Physics, Lahijan Branch, Islamic Azad University, Lahijan, Iran*

CuO doped zinc oxide particles were successfully prepared by sol-gel Pechini method at 500 °C. XRD and SEM techniques were used to characterize the CuO-doped ZnO samples. The photocatalytic degradation of nonylphenol polyethoxylate a nonionic surfactant was investigated in aqueous solution using CuO-ZnO nanoparticles. The degradation was studied under different conditions such as the Cu^{2+} concentration, amount of photocatalyst, irradiation time, pH, initial concentration and presence of electron acceptor. Under optimal degradation conditions of surfactant, the photodegradation percent of nonylphenol polyethoxylate was 91% when the solution was irradiated by the 400W high pressure mercury vapor lamp for five hour.

(Received June 6, 2014; accepted October 28, 2015)

Keywords: Synthesis, CuO-doped ZnO nanoparticles, Photocatalytic degradation, Nonylphenol polyethoxylate

1. Introduction

Recently, nano-sized semiconductor materials have attracted increasing attention to a wide range of possible applications such as photoelectric energy conversion materials [1–4] and water or air purification as friendly environmental photocatalysts [5–8]. In particular, ZnO has attracted much attention with respect to the degradation of various pollutants due to its being relatively cheap, stability and high photocatalysis [6–8]. One of the main problems associated with the feasibility and viability of ZnO semiconductor photocatalytic oxidation is represented by a high tendency of photoinduced hole–electron pairs to recombine, which implicates deactivation of the photocatalyst [9]. The most promising method to increase the photocatalytic efficiency is the surface modification of ZnO. The surface modification of ZnO can be achieved by metal doping into ZnO. A wide range of metal ions, in particular transition metal ions, have been used as dopants for ZnO because the recombination of photogenerated electrons and holes can be hindered by increasing the charge separation [10–13]. In order to make ZnO suitable with good efficiency, modification of ZnO by addition of another semiconductor has been used. In principle the coupling of different semiconductor oxides can reduce its band gap, extend its absorption range to visible light region, promote electron–hole pair separation under irradiation and, consequently, achieve a higher photocatalytic activity [14]. In the past several years, coupled semiconductors formed by ZnO and other metal oxides or sulfides such as TiO_2, SnO_2, Fe_2O_3, WO_3, CdS, ZnS and so on, have been reported [15–17], and there are also a lot of reports about CuO-ZnO nanocomposites presently [18, 19], however, most of them are used for the methanol synthesis, hydrogen production and gas sensor [20], and few used for photodegradation. In comparison with other oxide preparation methods, the polymerized complex method designed by Pechini [21] is a low temperature synthesis route which can produce a more uniform particle distribution. The polymeric precursors were prepared using zinc acetate and a mixed solution of citric acid and ethylene glycol as a chelating agent and reaction medium respectively. In this paper, we prepared the CuO-ZnO compound photocatalyst by “Pechini method” and then photocatalytic degradation of Nonylphenol Polyethoxylate (10 ethylene oxide unities, NP10EO), in the presence of CuO-ZnO nanopowder with UV light as the illuminate has been reported. The obtained results showed a good efficiency of nano-structured materials.

2. Experimental

The nonylphenol polyethoxylate having 10 ethoxy units (NP10-EO) was purchased from Merck Chemical Company. Zinc nitrate hexahydrate [$Zn(NO_3)_2{\cdot}6H_2O$], copper sulfate ($CuSO_4$.$5H_2O$), ethylene glycol, citric acid, $K_2S_2O_8$ and H_2O_2 were from Merck. All reagents were used as supplied by the manufacturers without further treatment.

2.1. Preparation of ZnO and CuO doped ZnO

Cu_x Zn_{1-x} O(x =0, 0.05, 0.1 and 0.15) powders were prepared by the sol–gel Pechini method, which has been used to synthesize polycationic oxide powders. The process is based on metallic citrate polymerization using ethylene glycol. A hydrocarboxylic acid, such as citric acid, is used to chelate cations in an aqueous solution. The addition of ethylene glycol leads to the formation of an organic ester. Polymerizations, promoted by heating the mixture, results in a homogeneous resin in which metal ions are uniformly distributed throughout the organic matrix. Zinc nitrate $[Zn(NO_3)_2 \cdot 6H2O]$ and copper sulphate powders are chosen as starting materials. Two solutions were prepared by dissolving separately measured amount of zinc nitrate and citric acid into 25mL ethylene glycol and deionized water. The concentration of the as prepared solutions was chosen to be 0.4 M. After complete dissolution of the precursors, citric acid solution was added to zinc nitrate solution and then chelated in with magnetic stirring at 80 ˚C. After 30 min copper sulphate was added in to solution as dopant material. The dopant stoichiometry was controlled by dissolving proper amount of copper sulphate. The Cu/Zn ratio in solution was changed from 0 to 0.15. The obtained mixture was stirred at 80 ˚C for 4 h to yield a clear and homogeneous solution. Afterwards sols were slowly cooled in air down to room temperature and then aged for 24 h in that situation. Following this, the samples put into a tube furnace and annealed in air at 500 ˚C for 2 h. The powders X-ray diffraction (XRD) patterns of the samples were recorded by a BRUKER D8 ADVANCE X-ray diffractometer using Cu K^{-} radiation. Microstructures, morphologies and element content were investigated by a JSM-6700F scanning electron microscopy (SEM).

2.2. Evaluation of photocatalytic activity

Photocatalytic testing was conducted in a thermostatic cylindrical Pyrex reactor with a 50 mL capacity. A 400-W mercury lamp, with a major emission at 223 nm, was used as the UV light source. In a 50mL flask, 25mL of NP10-EO solution with an initial concentration range of 30 mg/L was placed. A known amount of CuO-ZnO nanopowder was added to the surfactant and oxidant. The solution pH was adjusted by diluted HCl and NaOH solutions. The mixture was irradiated with the UV lamp for 5 h. The aqueous suspension was magnetically stirred (speed of 80 rpm) throughout the experiment. 5mL samples were withdrawn on regular intervals of time and centrifuged. Absorbance of the supernatant solution was measured and returned to the reactor. The quantitative estimation of the surfactant was carried out using a UV-Vis spectrophotometer (Model Jenway 6405) at λ_{max}= 223nm. The degree of photodegradation (X) as a function of time is given by the following relationship:

$$X = (C_0 - C)/C_0$$

Where C_0 is the initial concentration of surfactant, and C the concentration of surfactant at time t.

3. Results and discussion

3.1. Characterization of CuO doped ZnO

XRD patterns of ZnO nanopowder doped with copper, (concentration from 0 to 15 at. %) are shown in Fig.1. For undoped sample the peaks associated to planes (100), (002), (101), (102), (110), (103) and (112) of the hexagonal wurtzite ZnO structure (JCPDS: 65-3411) are observed. ZnO usually grows along the (002) direction due to the low surface free energy of (002) plane [22]. The undoped sample has shown the highest (002) diffraction peak intensity while the peak intensities of the Cu doped samples decreased with doping concentrations, which indicates that an increase in doping concentration deteriorates the crystallinity of the nanopowders.

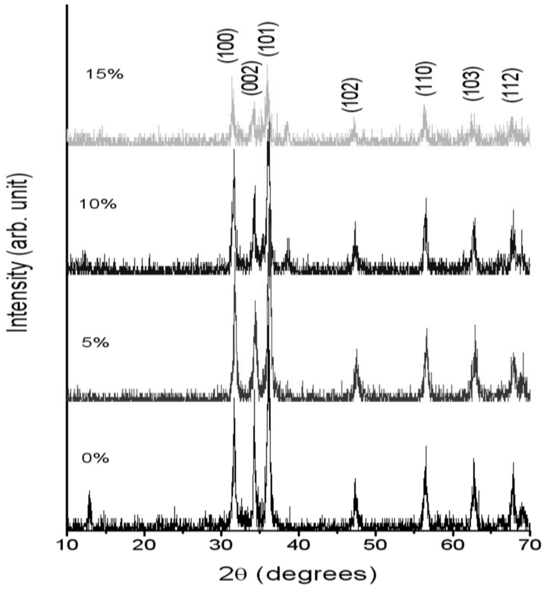

Fig. 1. XRD patterns of nanocrystalline CuO-ZnO powders at different Cu content

The crystallite size of the samples was estimated from the Scherrer's equation [23]:

$$D = \frac{k\lambda}{\beta cos\theta} \qquad (1)$$

Where D is crystallite size, λ is the X-ray wavelength used, β is the angular line width of half maximum intensity, θ is Bragg's diffraction angle and k is a constant. The average crystallite size associated to the (100), (002) and (101) directions was found to decrease from 20.39 nm (undoped) to a minimum of about 16.82 nm for a Cu concentration of 15 at. % (Table 1).

Table 1. Effect of copper concentration as a doping on the structural parameters of sol-gel pechini derived nanostructures ZnO powder.

Cu concentration (at. %)	FWHM (degrees)			D (nm)
	(100)	(002)	(101)	
0	0.39037	0.34205	0.4501	20.39
5	0.39198	0.45472	0.49326	17.93
10	0.41929	0.45805	0.4819	17.57
15	0.45112	0.46341	0.5045	16.82

SEM images of the nanocrystalline ZnO powder developed by Cu doping at different Cu contents are shown in Fig. 2. These SEM images show that the morphology of the samples is strongly dependent on the concentration of copper. A fairly single mode size distribution of grains are observed for undoped and 5 at. % doped powders. Generally, the low doping samples exhibited a porous microstructure and spherical crystalline surface particles. However, at 10 at. % Cu doped sample uneven surface and dense microstructure can be distinguished. Furthermore, when the doping concentration increases, the ZnO particle size decreases that testifies the XRD result. The change of particle size can be attributed to the almost 7% difference in ionic radius between zinc (0.074nm) and copper (0.069nm)

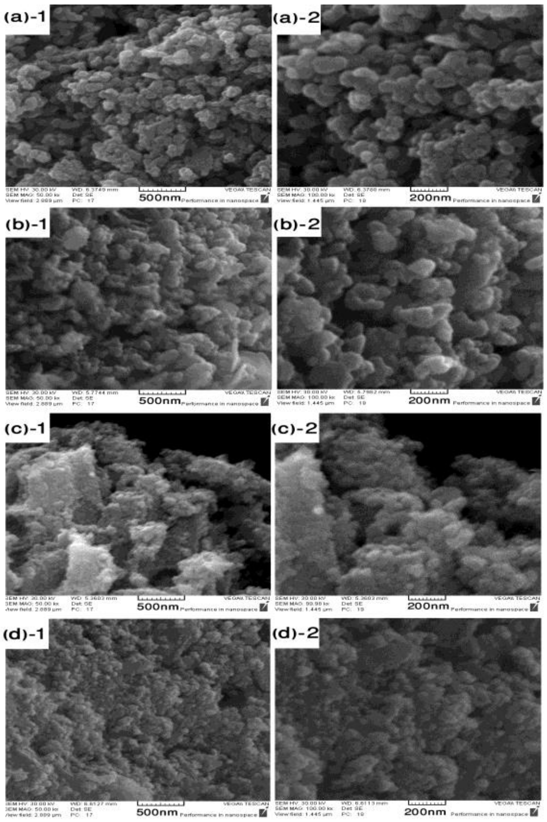

Fig. 2. SEM images of nanocrystalline CuO-ZnO powders at different magnifications. (a)-1,2: 0% Cu (b)-1,2: 5% Cu, (c)-1,2: 10% Cu and (d)-1,2: 15% Cu

3.2. Degradation of surfactant in the presence of a series of CuO-ZnO, and pure ZnO

The curves of NP10-EO degradation using ZnO and CuO-ZnO compounds prepared with different Cu^{2+} contents as photocatalysts are shown in Fig. 3. It is found that under UV light irradiation, all the CuO-ZnO compounds exhibit higher photocatalytic activity in degradation of NP10-EO than pure ZnO. It indicated that the addition of Cu had improved the absorption capability of ZnO toward UV light, possibly because when the particle diameter increased, the chance of recombination for photoinduced electron–hole pairs increased because of their slow arrival to reaction sites at the surface [24]. The best photocatalyst in degrading NP10-EO solution is 10% CuO-ZnO. The optimum degradation of NP10-EO is 91 % after 5 hours reaction.

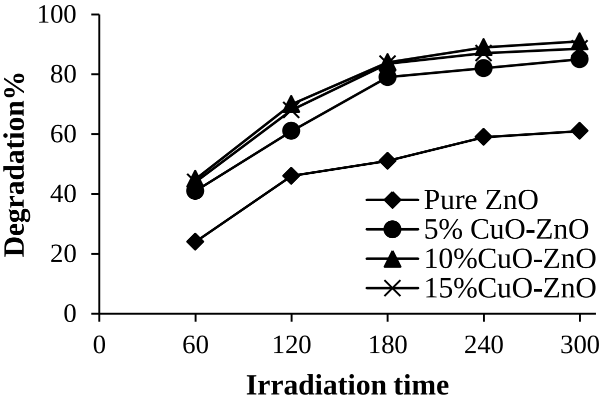

Fig. 3. Photocatalyzed degradation of NP10-EO in the presence of a series of CuO/ZnO, and pure ZnO. Conditions: $[NP10EO]_0$: 30mg/L, concentration of photocatalyst: 0.28 g/L, $K_2S_2O_8$=1mM, Irradiation time: 300 min, V_t:25mL.

3.3. Effect of UV, CuO-ZnO and $S_2O_8^{2-}$

The effect of sulfate radical ($SO_4^{\cdot-}$) as an oxidant on the degradation of NP10-EO was investigated and compared with UV (only), UV/ CuO-ZnO, UV/ $S_2O_8^{2-}$ and UV/ CuO-ZnO/ $S_2O_8^{2-}$ systems. As can be seen from Fig. 4 CuO-ZnO alone in the absence of sulfate radical and UV irradiation was found to have no measurable effect on the degradation of the surfactant during of 300 min irradiation time. A similar behavior was also observed in the UV system alone. In the case of sulfate radical alone, the degradation yield was determined as approximately 20% after 300min for 30 mg/L. The degradation yield of surfactant in UV/ $S_2O_8^{2-}$ system without CuO-ZnO was obtained approximately 23% after 300min treatment which is probably due to the production of radical species. The photocatalytic decomposition of peroxydisulfate potassium under UV radiation involves the formation of a number highly reactive radical ($OH^{\cdot}$, SO_4^{-}) and the non-radical species (O_3, SO_4^{2-}) [25, 26] as shown in Fig.4. UV/CuO-ZnO system had more significant effect on the degradation of surfactant than the UV/ $S_2O_8^{2-}$ system. This result is explained by the fact that CuO-ZnO is exposed to UV radiation; an electron is promoted from the valence band to the conduction band. Thus an h_{vB}^+/e_{CB}^- pairs is produced (Eq.(2)). The photocatalyst, CuO-ZnO, is a wide band gap semiconductor, corresponding to radiation in the near-UV rang:

$$\text{CuO-ZnO} + h\nu \rightarrow e_{CB}^- + h_{vB}^+ \quad (2)$$

The highly oxidative h_{vB}^+ can react easily with surface bound H_2O to produce hydroxyl radicals or can directly react with the surface adsorbed organic molecules (R) to from R^+ [27,28].

$$h_{vB}^+ + H_2O_{(ads)} \rightarrow OH^{\bullet} + H^+ \quad (3)$$

Surfactant + $OH^{\bullet}$ → degradation product (4)
Surfactant + CuO-ZnO (h_{vB}^+) → oxidation product (5)
Surfactant + CuO-ZnO (e_{CB}^-) → reduction product (6)

When potassium peroxydisulfate was added to UV/ CuO-ZnO system. Surfactant degradation increased from 49% to 91% after 300 min (Fig. 4).

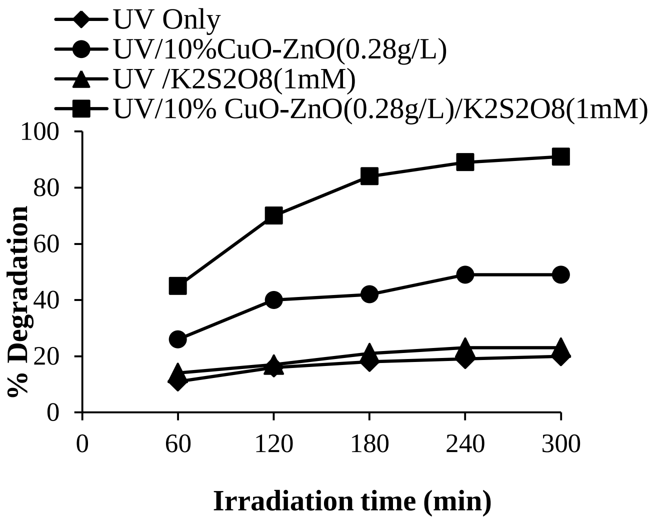

Fig. 4. Degradation of $[NP10EO]_0$=30 mg/L

3.4. Effect of amount of $K_2S_2O_8$

Acceleration in degradation rate of photocatalytic oxidation on CuO-ZnO occurs by photogenerated holes. It is shown that oxidation rate increases when recombination process is suppressed. Peroxydisulfate has been shown to be a more reliable and cheaper electron acceptor. The effect of peroxydisulfate as the electron acceptor was examined and is presented in Fig. 5.

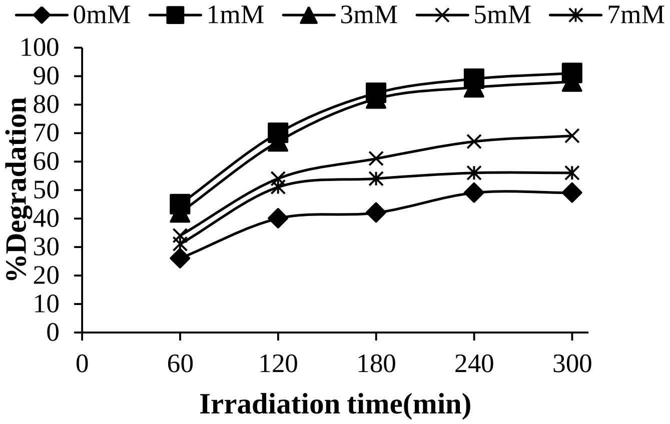

Fig. 5. Effect of $S_2O_8^{2-}$ concentration on the Degradation of NP10EO, Conditions: $[NP10EO]_0$= 30mg/L, 10%CuO-ZnO: 0.28 g/L, pH=6, V_t: 25 mL

The degradation of NP10EO was remarkably accelerated by addition of peroxydisulfate: 30 mg/L NP10EO and in the presence of 0.28 g/L CuO-ZnO was completely degraded under irradiation of 9 to 5 h in the absence and presence of 1 mM $K_2S_2O_8$ respectively.

$$\text{CuO-ZnO} + h\nu \rightarrow h^+ + e^- \quad (7)$$

$$h^+ + \text{NP10EO} \rightarrow (\text{NP10EO})^+ \quad (8)$$

$$e^- + S_2O_8^{2-} \rightarrow SO_4^{\bullet-} + SO_4^{2-} \quad (9)$$

The $SO_4^{\bullet-}$ radical is a strong oxidant, capable of mineralizing phenolic compounds such as butylated hydroxyanisole in water and the resulting SO_4^{2-} ion is not considered as a pollutant. The inhibition of reaction occurs at a high dosage of $S_2O_8^{2-}$ due to an increase in concentration of SO_4^{2-} ion (Eq. 9). The excess SO_4^{2-} ion is absorbed on the ZnO surface and reduces the catalytic activity. At the same time, the excess adsorbed SO_4^{2-} ion also reacts with the photogenerated holes (Eq. 10) and hydroxyl radicals (Eq. 11) [29].

$$SO_4^{2-} + h^+ \rightarrow SO_4^{\bullet-} \quad (10)$$

$$SO_4^{2-} + OH^{\bullet} \rightarrow SO_4^{\bullet-} + OH^- \quad (11)$$

3.5. Effect of catalyst concentration

In order to determine the effect of catalyst loading, the experiments were performed by varying catalyst concentration from 0.12 to 0.44 g/L for surfactant solutions of 30mg/L at pH 6. The degradation efficiency for various catalysts loading has been depicted in Fig. 6.

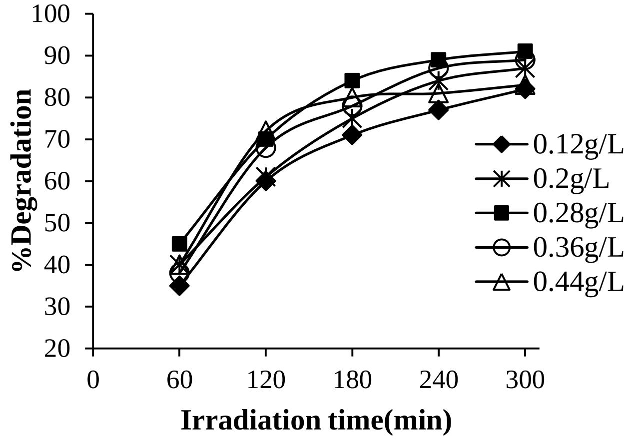

Fig. 6. Effect of catalyst concentration, Conditions: $[NP10EO]_0$ =30mg/L, $K_2S_2O_8$=1mM, pH=6, Irradiation time:300 min, V_t:25mL

It can be observed that the photodegradation efficiency increases with an increase in 10%CuO-ZnO concentration up to 0.28g/L, and is then decreased. This can be explained in terms of availability of active sites on the catalyst surface and the penetration of UV light into the suspension. The total active surface area increases with increasing catalyst weight. However, at the catalyst weight above optimum loading there is a decrease in UV light penetration due to screening effect of excess catalyst particle in the solution. Hence, the rate of photodegradation decreases at the higher catalyst loading [30].

3.6. Effect of concentration of surfactant

The influence of initial surfactant concentration on degradation was examined in the range 10–50mg/L at 0.28mg/L catalyst loading and $K_2S_2O_8$ (1mM) under UV irradiation. A representative concentration-time profile is shown in Fig. 7.

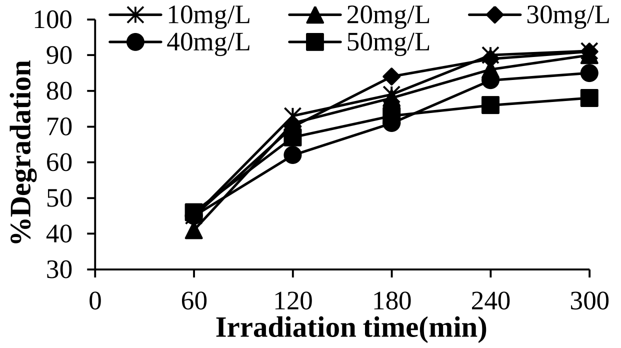

Fig. 7. Effect of initial surfactant concentration, Conditions: 10%CuO-ZnO: 0.28 g/L, $K_2S_2O_8$=1mM, pH=6, Irradiation time: 300 min, V_t: 25 mL

The rate of photodegradation of the surfactant decreased at higher concentrations. With increasing the amounts of surfactant, more surfactant molecules were adsorbed on the surface of the photocatalyst and the active sites of the catalysts were also reduced. Therefore, with increasing occupied sites of catalyst surface, the generation of hydroxyl radicals will be decreased. On the other hand, increasing concentration of surfactant can lead to decreasing the number of photons arrived to the surface of catalysts. By increasing the intensity of light adsorbed by molecules of surfactant, the excitation of photocatalyst particles by photons will be reduced leading to diminish in photodegradation efficiency [31].

3.7. Effect of pH

Photodegradation of surfactant was determined in a pH range of 2.0–11 in the presence of CuO-ZnO as catalyst (0.28g/L) and $K_2S_2O_8$(1mM).The results for irradiation time of 5 h are shown in Fig. 8. In all cases, the maximum degradation efficiency was obtained in pH 6.0 for NP10-EO. In presence of CuO-ZnO and in pH 6.0, degradation efficiency 91% is obtained. The interpretation of pH effects on the photocatalytic process is a very difficult task because of its multiple roles such as electrostatic interactions between the semiconductor surface, solvent molecules, substrate and charged radicals formed during the reaction process [32].

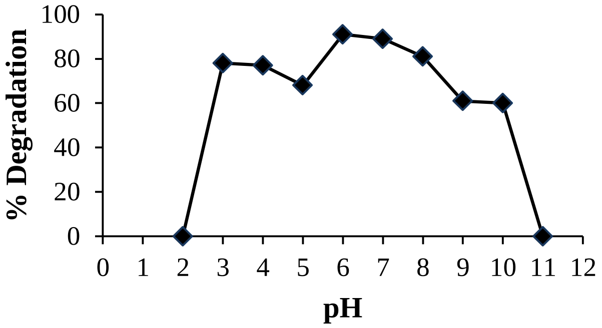

Fig. 8. Effect of pH, Conditions: $[NP10EO]_0$: 30mg/L, 10%CuO-ZnO: 0.28 g/L, $K_2S_2O_8$=1mM, Irradiation time: 300 min, V_t:25mL.

4. Conclusion

From literature it is well known that ZnO is a wide and a direct band gap material that has been shown to demonstrate photocatalytic activities. We therefore, synthesized CuO-doped ZnO nanocrystals for the first time using pechini method. The Pechini method is a promising alternative route or mixed oxide powder preparation. CuO-doped ZnO were examined for NP10EO degradation under UV irradiation. The particle size decreased with increasing Cu^{2+} concentration and the photocatalytic testing indicated that the 10% CuO-ZnO performed the best photocatalytic activity. The optimal degradation conditions of NP10EO are: 0.28 g/L catalyst, pH 6.0, 1mM $K_2S_2O_8$ and concentration of NP10EO

30mg/L. After 5 h irradiation about 91% removal of nonylphenol polyethoxylate was achieved.

Acknowledgment

The financial support provided by the Islamic Azad University of Lahijan is greatly acknowledged.

References

[1] Y. Murata, S. Fukuta, S. Ishikawa, S. Yokayama, Sol Energy Mater Sol Cells. **62**, 157 (2000).

[2] D. A. Tryk, A. Fujishima, K. Honda, Electrochem Acta. **45**, 2363 (2000).

[3] K. Ishibashi, A. Fujishima, T. Watanabe, K. Hashimoto, J. Photochem Photobiol A. **134**, 139 (2000).

[4] M. I. Litter, Appl Catal B. **23**, 89 (1999).

[5] E. Evgenidou, K. Futianos, I. Poulios, Appl Catal B. **59**, 81 (2005).

[6] N. C. Harihara.Preparation, Appl Catal A. **30**, 455 (2006).

[7] M. A. Behnajady, N. Modirshahla, R. Hamzayi, J Hazard Mater. **133**, 226 (2006).

[8] R-Y. Hong, T-T.Pan, J-Z. Qian, H-Z. Li, Chem Eng J. **119**, 71 (2006).

[9] H. Gerisher, A. Heller, J Electrochem Soc. **139**, 113 (1992).

[10] M. Height, S. Pratsinis, O. Mekasuwandumrong, P. Praserthdam, Appl. Catal. B: Environ. **63**, 305 (2006).

[11] C. Chen, Z. Wang, S. Ruan, B. Zou, M. Zhao, F. Wu, Dyes Pigm. **77**, 204 (2008).

[12] R. Ullah, J. Dutta, J. Hazard. Mater. **156**, 194 (2008).

[13] H. Wang, C. Xie, W. Zhang, S. Cai, Z. Yang, Y. Gui, J. Hazard. Mater. **141**, 645 (2007).

[14] R. M. Mohamed, I. A. Mkhalid, J. Alloys Compd. **501**, 301 (2010).

[15] M. Giahi, H. Taghavi, S. Habibi, Russ. J. Phys. Chem. A. **86**, 81 (2012).

[16] M. Giahi, S. Habibi, S. Toutounchi, M. Khavei, Russ. J. Phys. Chem. A. **86**, 689 (2012).

[17] K. Byrappa, A. K. Subramani, S. Ananda, K. M. L Rai, M. H. Sunitha, B. Basavalingu, K. Soga, J. Mater. Sci. **41**, 1355 (2006).

[18] I. Eswaramoorthi, V. Sundaramurthy, A. K. Dalai, Appl. Catal. A. **313**, 22 (2006).

[19] H. C. Yang, F. W. Chang, L. S. Roselin, J. Mol. Catal. A. **276**, 184 (2007).

[20] G. Fierro, M. Lo Jacono, M. Inversi, P. Porta, F. Cioci, R. Lavecchia, Appl. Catal. A. **137**, 327 (1996).

[21] M. I. B. Bernardia, L. E. Soledadea, I. A. Santosb, E. R. Leitea, E. Longoa, J. A. Varelac, Thin Solid Films. **405**, 228, (2002).

[22] Y. Morinaga, K. Sakuragi, N. Fujimura, T. Ito, J. Crystal Growth. **174**, 691 (1997).

[23] B. D. Cullity and S. R. Stock, Elements of X-ray Diffraction, 3rd ed., Prentice Hall, Inc., New Jersey, USA, 2001, p. 167.

[24] L. Q. Jing, Z. L. Xu, X. J. Sun, J. Shang, W. M. Cai, Appl. Surf. Sci. **180**, 308 (2001).

[25] C. Lee, J. Yoon, J. photobiol. A: Chem. **165**, 35 (2004).

[26] I. K. Konstantinous, T. A. Alabanis, Appl. Catal. B: Environ. **49**, 1 (2009).

[27] J. Gimenz, D. Curco, P. Marco, water Sci. Technol. **35**, 207 (1997).

[28] C. G. da Silva, J. L. Faria, J. Photochem. Photobiol. A: Chem. **155**, 133 (2003).

[29] N. Romero, J. Blanco, B. Sanchez, A. Vidal, S. Malato, A. I. Cardona, E. Garcia, Solar Energy. **66**, 169 (1999).

[30] J. M. Hermann, Catal. Today, **53**, 115 (1999).

[31] B. Rohe, W. S. Veeman, M. Tausch, Nano Technol. **17**, 277 (2006).

[32] U. G. Akpan, B. H. Hameed, J Hazard Mater. **170**, 520 (2009).

---

*Corresponding author: giahi_m@yahoo.com